processes

Article

Acid System and Stimulation Efficiency of Multistage Acid Fracturing in Porous Carbonate Reservoirs

Dawei Zhu [1,*], Yunjin Wang [2,*], Mingyue Cui [1], Fujian Zhou [2], Yaocong Wang [3], Chong Liang [1], Honglan Zou [1] and Fei Yao [1]

1 Research Institute of Petroleum Exploration & Development, PetroChina, Beijing 100083, China
2 State Key Laboratory of Petroleum Resources and Prospecting, China University of Petroleum (Beijing), Beijing 102249, China
3 Oil & Gas Technology Research Institute, Petrochina Changqing Oilfield Company, Xi'an 710018, China
* Correspondence: zhudawei69@petrochina.com.cn (D.Z.); yunjingwang112@foxmail.com (Y.W.)

Abstract: With little to no natural fracture development and the high calcite content in porous carbonate reservoirs, for multistage acid fracturing, different fluids are used to form a viscous fingering in the fracture, thus enhancing the degree of nonuniform etching. However, existing studies on multistage acid fracturing mainly focused on the combination of fracturing fluid and acid, which is less specific for porous carbonate rocks. Here, the rheological properties of five fluids, including guar-based fluid, cross-linked guar, gelled acid, cross-linked acid, and diverting acid, were studied at each temperature condition, and the viscosity relationship between each fluid was clarified. Based on the rheological properties, the differences between the seven liquid combinations on the etched morphology of the fracture walls were studied and analyzed. The conductivity of the seven acid-etched fractures under different closure stress was simulated. The experimental results showed that the viscosity relationships between the fluids at different temperatures were cross-linked guar > cross-linked acid > diverting acid (spent acid) > gelled acid > guar-based liquid > diverting acid (fresh acid). Because cross-linked acid has higher viscosity than gelled acid, it can form more obvious viscous fingering with a variety of liquids, which is more suitable for acid fracturing stimulation of porous carbonate reservoirs. In addition, the combination of cross-linked and diverting acids was screened out. The multistage alternate injection of this fluid combination could form tortuous and complex etching channels, and its acid-etching fracture conductivity was significantly higher than that of other fluid combinations at different closure stress. In this study, we optimized the fluid combination of porous carbonates and clarified the effect and mechanism of nonuniform etching to provide guidance for the fluid combination selection of multistage alternate acid fracturing process for porous carbonate reservoirs.

Keywords: multistage acid fracturing; porous carbonate reservoir; morphology; conductivity; acid combination

Citation: Zhu, D.; Wang, Y.; Cui, M.; Zhou, F.; Wang, Y.; Liang, C.; Zou, H.; Yao, F. Acid System and Stimulation Efficiency of Multistage Acid Fracturing in Porous Carbonate Reservoirs. *Processes* **2022**, *10*, 1883. https://doi.org/10.3390/pr10091883

Academic Editors: Linhua Pan, Yushi Zou, Jie Wang, Minghui Li, Wei Feng and Lufeng Zhang

Received: 23 August 2022
Accepted: 11 September 2022
Published: 17 September 2022

1. Introduction

Porous carbonate reservoirs generally have low porosity and permeability, high calcite content in rock minerals, and the natural fractures are less or even not developed [1,2]. This type of reservoir is especially developed in the Middle East or central Asia [3]. Acid fracturing is one of the most effective measures for carbonate stimulation [4,5]. The acid-etching fracture conductivity after acid fracturing treatment is a key factor affecting oil and gas production, and is a key parameter in the acid fracturing design of carbonate reservoirs [6,7]. Due to the characteristics of porous carbonate with pure lithology, nonuniform etching is not easily formed by the conventional acid fracturing process [8,9]. Multistage alternate acid fracturing is widely used to enhance the degree of nonuniform etching, and was proven to be the most effective stimulation measure for porous carbonates [10].

Early multistage alternate acid fracturing technology is mainly a combination of fracturing fluid and acid fluid [11,12]. The main advantages of adding fracturing fluid to the acid fracturing process include: (1) the use of highly viscous fracturing fluid to plug the natural fractures in the reservoir and the wormhole formed in the fracture wall, thus reducing the filtration of acid through the natural fractures and fracture wall and increasing the volume of fractures during acid fracturing [13,14]; (2) the viscosity of the fracturing fluid is usually higher than that of the acid fluid, and the difference in viscosity between the alternately injected fracturing fluid and the acid fluid makes the two fluids form viscous fingering in the fracture [15]. This viscous fingering causes the distribution of the acid to be nonuniform in the fracture, thus producing nonuniform etching on the fracture wall. The formation of these nonuniform etchings prevents the fracture from completely closing under high closure stress and maintains a good oil and gas flow channel [16]. Notably, cross-linked guar is usually a chain compound formed by cross-linking of hydroxypropyl guar under alkaline conditions and the cross-link agent, thereby increasing the viscosity of the fracturing fluid [17]. Under acidic conditions, the cross-linking structure is destroyed, and the viscosity of the fluid is significantly reduced and may even be lower than that of the gelled and cross-linked acids [18]. To solve this problem, researchers have developed acid-resistant polymeric fracturing fluids that can effectively improve the fluid viscosity of fracturing fluids in highly acidic environments [19]. However, such fracturing fluids are costly, and their application in the field is limited.

Gelled and cross-linked acids are often used in multistage acid fracturing because of their higher viscosity than those of other acid systems, which can effectively reduce acid filtration and open the reservoir to form fractures [20]. In recent years, with the development of acid systems, the combination of fluid systems for multistage acid fracturing has also changed, such as the combination of fracturing fluid and gelled acid, and diverting acid and gelled acid [21,22]. The viscosity of fresh diverting acid is lower and consistent with that of water. As H^+ is consumed during the acid–rock reaction and carbonate minerals are dissolved, the pH and Ca^{2+} concentration increase in the solution. Surfactants in the diverting acid are entangled to form micelles in weakly acidic environments with metal ions, and the presence of micelles greatly enhances the viscosity of the acid solution [23]. Fresh low-viscosity acid has good flow ability in fractures, while spent high-viscosity spent acid can effectively plug the natural fractures and wormholes to reduce acid filtration [1]. Current research on porous carbonates has focused on two acid systems: gelled acid and cross-linked acid, and stimulation parameters such as injection rate and injection time. However, the stimulation effect and mechanism of the combination of diverting acid and other acid fluids on porous carbonate are still unclear.

In this study, a diverting acid whose viscosity gradually increases with reaction time was introduced. Considering the temperature variation, the rheological properties of five fluid systems at different temperatures were studied, and the viscosity relationship between the fluids was clarified. Based on the combinations of fracturing fluid and acid in conventional acid fracturing, we introduced combinations of acids. The conductivities of acid-etching fractures for different acid combinations were studied. The acid fracturing stimulation efficiencies of different acid combinations were clarified, and the fluid combinations suitable for porous carbonate reservoirs were preferably selected.

2. Experiment Preparation

In the process of acid fracturing, the acid uniformly reacts with the carbonate minerals on the fracture wall, hindering nonuniform etching on the fracture wall. With the completion of acid fracturing and the progression of oil and gas flowback, the pore pressure of the reservoir gradually decreases and the closure stress gradually increases in the reservoir. Uniformly etched fractures rapidly close under closure stress, and the conductivity is difficult to maintain, which seriously affects the acid fracturing effect. Multistage acid fracturing stimulation can reasonably use the reactions and rheological characteristics of the acid, which make the acid produce viscous fingering in the fracture, thus producing nonuniform etching on the fracture wall, finally forming a connected high-permeability oil and gas channel.

2.1. Rock Slab Preparation

Indiana limestone cores were analyzed by XRD, and the mineral composition of the cores was mainly calcite (93.7%) and dolomite (7.3%). In addition, the porosity and permeability of the Indiana limestone were 20.1% and 7.2 mD, respectively. The cores used in the experiment were processed with by wire cutting technology into a 178 mm long, 19 mm arc rock slab that was 38 mm wide and 50 mm high (Figure 1), which ensured the rock slab size fully matched the size of API acid etching conductivity chamber.

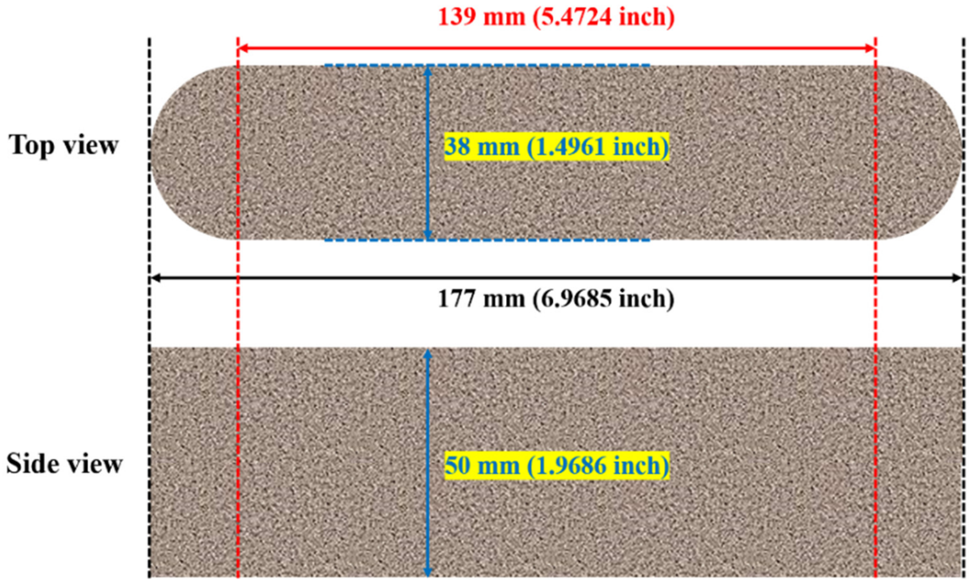

Figure 1. The size of the limestone slab.

2.2. Fluid Preparation

In this work, five kinds of liquid systems were used in the multistage acid fracturing experiment, including a guar-based solution, cross-linked guar, gelled acid, cross-linked acid, and diverting acid. The specific formulas of the liquids were as follows:

(1) Guar-based solution: 0.27 wt% HPG + 0.1 wt% fungicide, and 0.3 wt% clay stabilizer;

(2) Cross-linked guar: 0.27 wt% HPG + 0.1 wt% fungicide + 0.3 wt% clay stabilizer, and 0.3 wt% cross-link agent;

(3) Gelled acid: 20 wt% HCl + 0.6 wt% gelling agent, and 1.5 wt% corrosion inhibitor;

(4) Cross-linked acid: 20 wt% HCl + 0.6 wt% gelling agent + 0.6 wt% cross-link agent, and 1.5 wt% corrosion inhibitor;

(5) Diverting acid: 20 wt% HCl + 1.5 wt% corrosion inhibitor, and 7 wt% diverting agent.

In the reaction of diverting acid with carbonate minerals, the viscosity of the spent diverting acid solution gradually increases under environments with high pH and Ca^{2+} concentration, eventually achieving the purpose of uniform acidizing. After the chemical reaction between fresh acid and carbonate minerals at the fracture wall during acid fracturing, the highly viscous spent acid enters the porous medium through the fracture wall. The highly viscous spent acid, by entering the porous media, can enhance the percolation resistance of the subsequent acid into the fracture wall, thus reducing acid loss and improving fracturing efficiency. Therefore, in addition to the viscosity of the fresh diverting acid, the viscosity of the spent diverting acid was also tested in this study. The preparation process of the spent diverting acid was as follows: (1) 200 mL of 15 wt% HCl solution was prepared by using deionized water and 37 wt% HCl. (2) We added 1.5 wt% corrosion inhibitor to the removed liquid and 7 wt% diverting agent, which is a kind of

Gemini quaternary ammonium salt cationic surfactant. (3) Excessive Ca_2CO_3 was added to the water bath at 50 °C to ensure the HCl fully reacted, and the solution after the reaction was centrifuged at 3000 r/min to obtain the supernatant.

2.3. Experiment Apparatus

In this work, an acid etching fracture conductivity testing system (Figure 2) was used, which consisted of a liquid rheology testing device, an acid etching simulation device, a conductivity testing device, and a 3D laser scanning device. The rheology testing device was made of Hastelloy and was able to test the viscosity of fracturing fluid and acid at different temperatures [24]. The acid etching simulation device was used to etch the rock slab by injecting acid, thus simulating the process of etching the fracture wall during acid fracturing. The conductivity testing device was used to test the flow conductivity of the fracture at different closure stresses, thus objectively reflecting the closure of the acid-etching fracture at different closure stresses. The 3D laser scanning device was used to visualize the acid etching on the fracture walls.

Figure 2. Acid fracturing conductivity test system.

2.4. Experimental Procedure

The main procedures of the acid rheology and acid etching slab conductivity testing experiments are described below:

(1) Determination of the rheological properties of the acid solution: the viscosity of the acid system used in the experiment was measured at different temperatures using the Harker rheometer to clarify the viscosity relationship of each acid system at the target temperature.

(2) Acid etching of fracture surfaces: A pair of smooth rock slabs was installed parallel to the reaction chamber of the acid-etching simulation device and began to heat up. The back pressure was set to 7 MPa during the experiment. When the ambient temperature was heated to the experimentally set value, the acid was pumped into the fracture in the reaction chamber according to the experimental scheme, and the pumped acid chemically reacted with the rock minerals on the fracture wall.

(3) Scanning the surface morphology of the fracture after acid etching: After the reaction, the acid-etched rock slab was removed from the acid etching simulation device, and the surface of the rock slab was cleaned of the acid and residue after the reaction using deionized water. The surface morphological features of the acid-etching fractures were obtained using a 3D laser scanning device.

(4) Testing the flow conductivity of acid-etching fractures: The reacted rock slabs were installed parallel in the conductivity chamber of the conductivity testing device, and the initial closure stress was applied at 5 MPa to make the two rock plates contact. Deionized water was injected at a flow rate of 5 mL/min. After the flow rate at the outlet of the device stabilized at 5 mL/min, the closure stress was increased according to the experimental plan to determine the conductivity at different closure stresses.

3. Result and Discussion

3.1. Liquid Rheology Test Result

By using a liquid rheology testing device, the viscosity of the liquids at room temperature was measured by shearing the six liquids at a constant speed for 30 min. Then, the ambient temperature was slowly raised until the temperature rose to 90 °C, which was then stabilized at 90 °C, and the liquid was continuously sheared for 60 min. After the viscosity of the liquid was stable, the average viscosity of the viscosity stable period was taken as the viscosity of the liquid at 90 °C. The shear rate was kept at 170 s^{-1} during the experiment. The rheological results of the six liquids are shown in Figure 3. As can be seen from the figure, the viscosities of the guar-based fluid, cross-linked guar, gelled acid, cross-linked acid, and spent diverting acid were 86.4, 867.3, 98.3, 394.8, and 420.6 mPa·s, respectively, at room temperature. The viscosities of all acid systems gradually decreased as the ambient temperature continued to rise. At 90 °C, the viscosities of the guar-based solution, cross-linked guar, gelled acid, cross-linked acid, and spent diverting acid were 51.6, 391.9, 28.9, 136.4, and 72.7 mPa·s, respectively. This viscosity change trend was consistent with those reported in previous studies [25,26]. The viscosity of the cross-linked guar always remained the highest at all temperature conditions, followed by that of the cross-linked acid and spent diverting acid, and the viscosities of the guar-based solution and gelled acid were the smallest and least different. The viscosity of the fresh diverting acid was 2.7 mPa·s due to the characteristics of the diverting acid, and slightly decreased as the ambient temperature kept increasing.

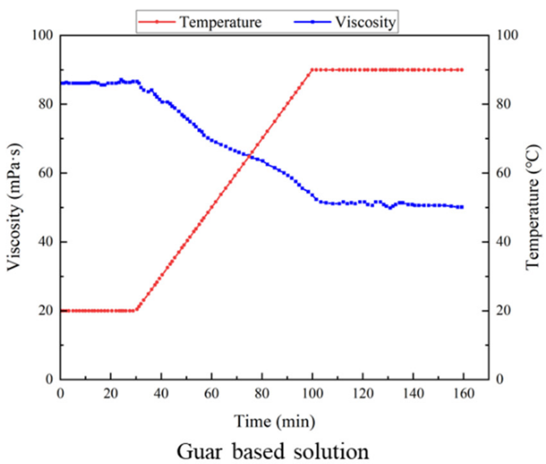

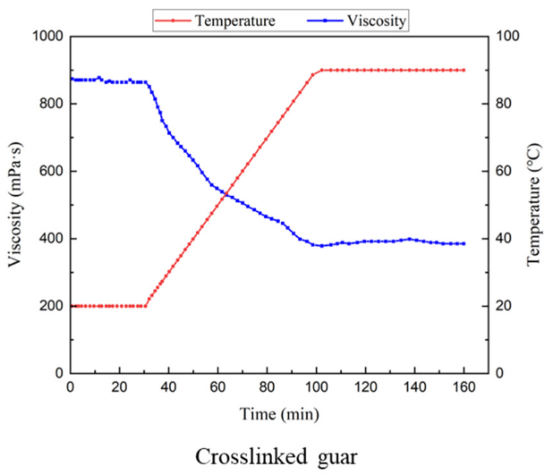

Figure 3. *Cont.*

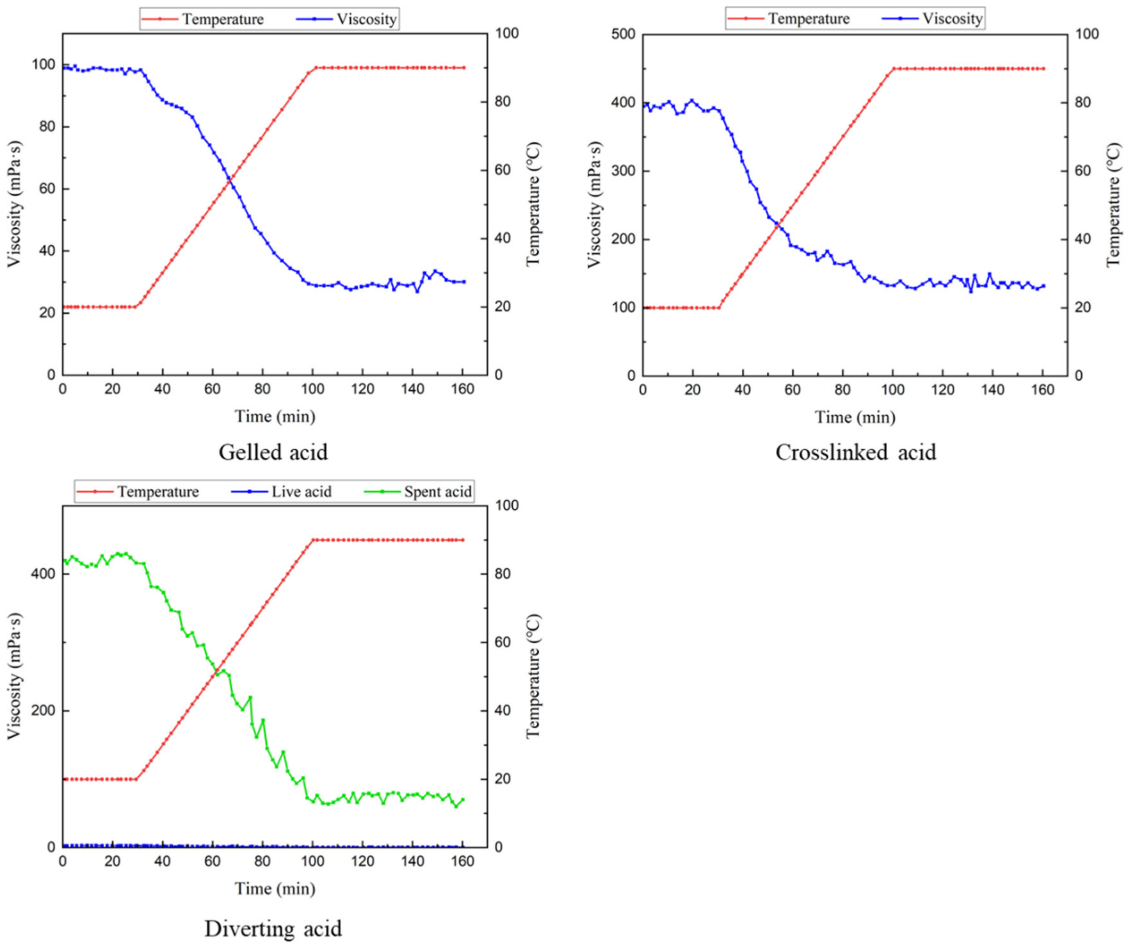

Figure 3. The viscosity of five acid systems at different temperatures.

3.2. Acid Etching Simulation Result

According to the optimization principle of multistage acid fracturing in carbonate reservoirs, seven combinations of five fluids were considered to study the effect of acid etching on the fracture wall of carbonate rocks under different fluid combinations. To ensure that the total amount of acid injected in the multistage acid fracturing process was consistent, the injection time in the multistage acid fracturing was adjusted, and the specific experimental arrangement is shown in Table 1. The ambient temperature was maintained at 90 °C during the experiments. Combined with the injection rate during acid fracturing treatment in the field and previous research results [21], the injection rate in the experiment was set to 30 mL/min.

The results of the rock slab acid etching simulation are shown in Figures 4 and 5. As can be seen from the figures, the surfaces of the rock slab after both multistage alternate injection of the guar-based solution and gelled acid and multistage alternating injection of gelled acid and diverting acid were both relatively smooth. This uniform etching completely closed the fractures under high closure stress, thus reducing the acid fracturing effect. There was nonuniform etching on the rock slab after multistage alternating injection of the cross-linked acid and guar-based solution, but the degree of nonuniform etching was lower. More obvious [27,28] etching grooves formed after multistage alternating injection of gelled acid and cross-linked guar, cross-linked acid and gelled acid, and cross-linked acid and cross-linked guar. This etched groove greatly enhanced the nonuniform etching degree of the fracture wall [29], which hindered the acid-etched fracture from completely closing under the closing pressure after the acid fracturing stimulation, thus forming a high-speed channel for the flow of oil and gas. The etched grooves formed after the multistage alternate injection of cross-linked acid and diverting acid were more obvious. These grooves greatly enhanced the degree of nonuniform etching on the fracture walls: tortuous and complex grooves were harder difficult to close under closure stress. In addition, the slab overall showed a greater degree of dissolution at the entrance, and the degree of dissolution from the entrance to the exit showed a gradually decreasing trend. This is because the acid concentration at the point of entry into the fracture was higher, which created a more intense acid–rock reaction, and the degree of etching was correspondingly higher. With the consumption of H^+ in acid by the acid–rock reaction, the concentration of acid at the exit was lower, and, thus, the degree of reaction was relatively weaker.

Table 1. Multistage acid fracturing test arrangement and conductivity test results.

Liquid Combination	Stage	Injection Time	Injection Fluid	Conductivity (D·cm) 15 MPa	30 MPa	45 MPa	60 MPa	75 MPa
Guar-based fluid (GB) and gelled acid (GA)	1	20 min	GB	98.5	51.3	22	7.4	1.3
	2	20 min	GA					
	3	20 min	GB					
	4	20 min	GA					
	5	20 min	GB					
	6	20 min	GA					
Cross-linked guar (CA) and gelled acid (GA)	1	20 min	CA	312.7	143.7	56.2	21.3	10.8
	2	20 min	GA					
	3	20 min	CA					
	4	20 min	GA					
	5	20 min	CA					
	6	20 min	GA					
Gelled acid and (GA) diverting acid (DA)	1	10 min	GA	154.4	81.4	24.3	11.2	6.7
	2	10 min	DA					
	3	10 min	GA					
	4	10 min	DA					
	5	10 min	GA					
	6	10 min	DA					
Guar-based fluid (GB) and cross-linked acid (CA)	1	20 min	GB	356.1	140	48.3	16.1	5.1
	2	20 min	CA					
	3	20 min	GB					
	4	20 min	CA					
	5	20 min	GB					
	6	20 min	CA					
Cross-linked guar (CG) and cross-linked acid (CA)	1	20 min	CG	217.2	97.3	49.7	20.1	5.3
	2	20 min	CA					
	3	20 min	CG					
	4	20 min	CA					
	5	20 min	CG					
	6	20 min	CA					
Cross-linked acid (CA) and gelled acid (GA)	1	10 min	CA	342.1	164.2	61.7	20.3	10.1
	2	10 min	GA					
	3	10 min	CA					
	4	10 min	GA					
	5	10 min	CA					
	6	10 min	GA					
Cross-linked acid (CA) and diverting acid (DA)	1	10 min	CA	514.2	314	148.3	73.4	41.2
	2	10 min	DA					
	3	10 min	CA					
	4	10 min	DA					
	5	10 min	CA					
	6	10 min	DA					

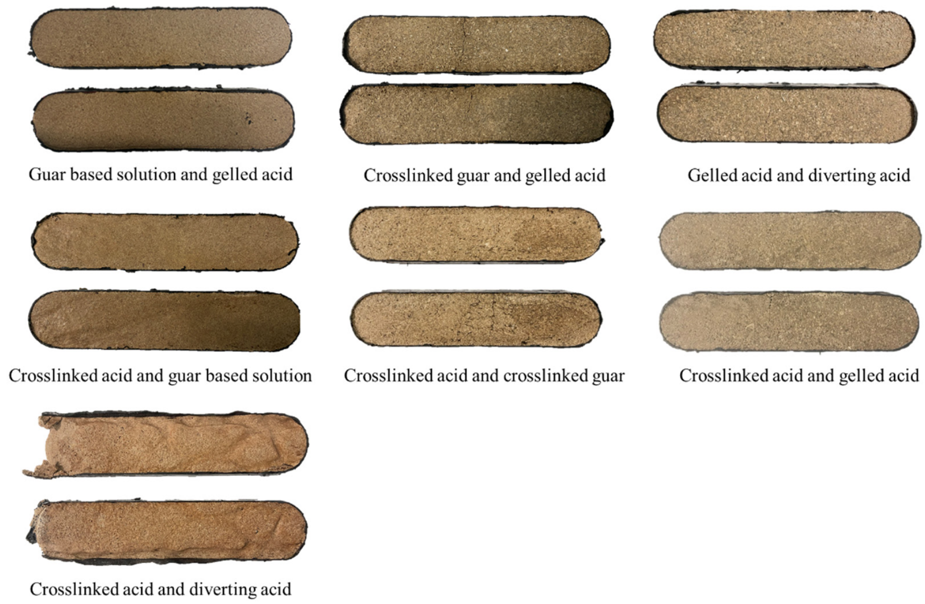

Figure 4. Surface morphology of slabs after acid etching.

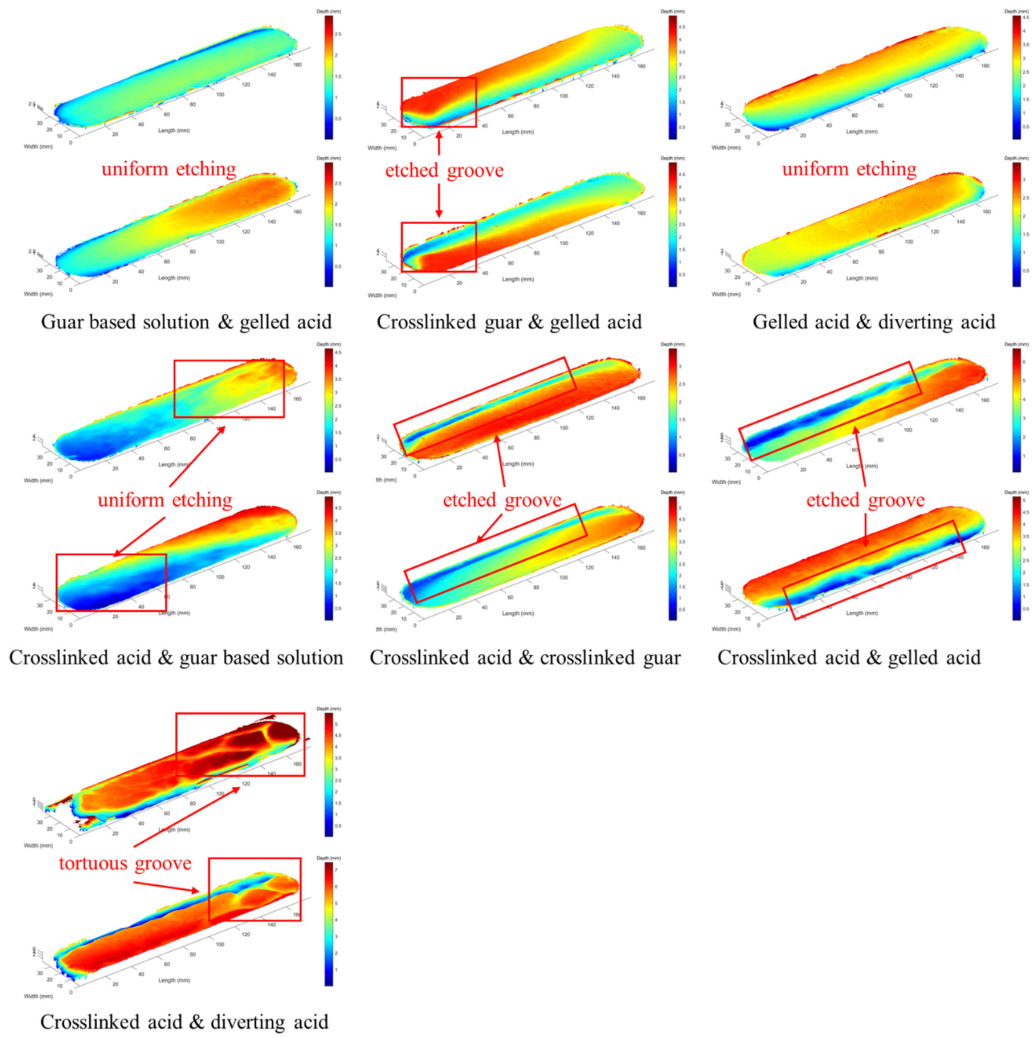

Figure 5. Surface scan of slabs after acid etching.

3.3. Conductivity Test Result

The fracture conductivity of the rock slabs, after acid etching with different acid combinations, was tested under closing pressures of 15, 30, 45, 60, and 75 MPa using the conductivity testing device, and the test results are shown in Figure 6. From the conductivity test results, we found that the fracture conductivity after cross-linked acid etching was generally higher than that after gelled acid etching. This is because the viscosity of cross-linked acid was five times higher than that of gelled acid at 90 °C, and its viscosity difference with guar-based fluid and diverting acid was even larger. Previous studies [30] showed that viscosity differences can make low-viscosity fluid form viscous fingering in high-viscosity fluid, and this viscous fingering can make the distribution of the acid nonuniform in the fracture, thus achieving nonuniform etching on the fracture wall, which greatly enhances the fracture conductivity under high closure stress. Notably, the multistage alternate injection of cross-linked acid and diverting acid had significantly higher conductivities than the other acid combinations at each closure stress. The combination of cross-linked acid and diverting acid had a conductivity of 514.2 D·cm at a closure stress of 15 MPa. The conductivity gradually decreased as the closure stress increased, and had a conductivity of 148.3 D·cm at a closure stress of 45 MPa. When the closure stress was 75 MPa, the conductivity of the acid-etched fracture was 41.2 D·cm. Combined with the acid rheology test and rock slab etching results, we determined that this was due to the large difference in viscosity between the cross-linked acid and the diverting acid, which led to more obvious viscous fingering of the acid inside the fracture. This obvious viscous fingering caused the acid etching of the fracture wall to form a tortuous and complex etching channel. Such channels cannot be completely closed even under high closure stress, which provides better flow channels for the oil and gas production process and greatly enhances the effect of acid fracturing stimulation in carbonate reservoirs.

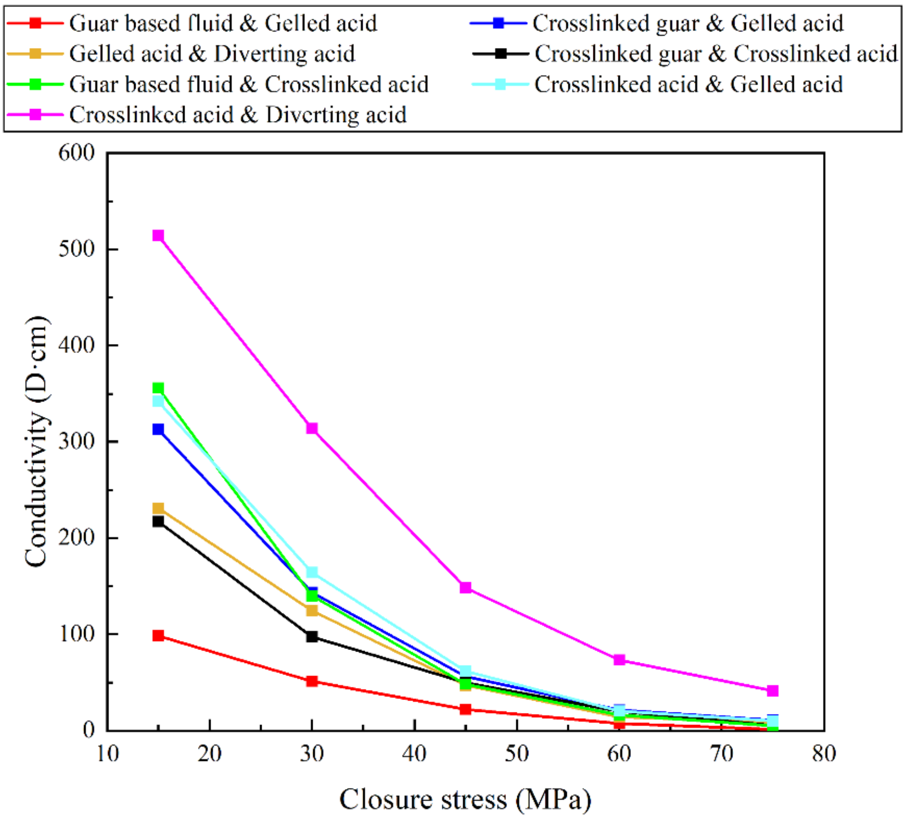

Figure 6. Conductivity under multistage alternate injection of different fluid combinations.

In summary, the fracture conductivity after etching with cross-linked acid is generally higher than that of etching with gelled acid. This is because the viscosity of cross-linked acid at 90 °C is five times higher than that of gelled acid, and its viscosity difference with guar-based fluid and diverting acid is even larger. The viscosity difference can make the acid produce viscous fingering in the fracture. This viscous fingering can make the distribution of the acid nonuniform in the fracture, thus achieving the nonuniform etching of carbonate minerals on the fracture wall. The combination of cross-linked acid and diverting acid can form tortuous and complex etching channels on the fracture wall due to their large difference in viscosity, which can improve the efficiency of acid fracturing.

4. Conclusions

In this study, the rheological properties of a guar-based solution, cross-linked guar, gelled acid, cross-linked acid, and diverting acid were investigated at different temperatures. Multistage acid fracturing experiments were carried out using different acid combinations, and the effects of different multiple-acid systems on the nonuniform etching of the fracture wall were systematically investigated. The relationship between the surface morphology and the conductivity of the acid-etched fracture was analyzed. Based on the experiment results and discussion, the following conclusions were obtained:

(1) The viscosity of all five acid fracturing working fluids gradually decreased with the increase in temperature. At different temperatures, the viscosity relationships were: cross-linked guar > cross-linked acid > diverting acid (spent acid) > gelled acid > guar-based solution > diverting acid (fresh acid).

(2) Cross-linked acid is more suitable for acid fracturing stimulation of carbonate reservoir than gelled acid. Due to the high viscosity of cross-linked acid and the large difference in viscosity with many other liquids used in acid fracturing stimulation, the combination of cross-linked acid with other liquids effectively produce viscous fingering in the fracture. This viscous fingering means the cross-linked acids generally have higher fracture conductivity than gelled acids after acid etching.

(3) The combination of cross-linked acid and diverting acid is most effective for multistage acid fracturing stimulation of carbonate reservoirs. The liquid combination of cross-linked acid and diverting acid has a large difference in viscosity and can form tortuous and complex etched channels in the fracture walls, which do not completely close even at high closure stress. When the closure stress was 75 MPa, the acid-etched fracture still had a conductivity of 41.2 D·cm.

Nonuniform acid fracturing in porous carbonatite is still a worldwide problem. In this work, we evaluated and compared the effects of various liquid combinations on multistage acid fracturing, and proposed that the combination of diverting acid and cross-linked acid can effectively improve the degree of nonuniform etching in the fracture. However, when the environmental temperature is above 90 °C, the performance of the diverting acid is seriously reduced. Therefore, the performance of diverting acid in high-temperature reservoirs must be improved. In addition, under normal conditions, the viscosity of the acid solution is controllable within a certain range, and the effect of the viscosity relationship between the diverting acid and the cross-linked acid on the acid fracturing effect still needs further study.

Author Contributions: Writing—original manuscript, D.Z.; experiment, Y.W. (Yunjin Wang) and Y.W. (Yaocong Wang); supervision, M.C. and F.Z.; investigation, C.L.; data curation, H.Z.; formal analysis, F.Y. All authors have read and agreed to the published version of the manuscript.

Funding: This research was funded by the National Natural Science Foundation of China (No. 52174045), the CNPC "Fourteenth Five Year Plan" science and technology projects (No. 2021DJ3405).

Conflicts of Interest: The authors declare no conflict of interest.

References

1. Zhu, D.; Wang, Y.; Cui, M.; Zhou, F.; Zhang, Y.; Liang, C.; Zou, H.; Yao, F. Effects of spent viscoelastic-surfactant acid flow on wormholes propagation and diverting performance in heterogeneous carbonate reservoir. *Energy Rep.* **2022**, *8*, 8321–8332. [CrossRef]
2. Li, M.-H.; Zhou, F.-J.; Liu, J.-J.; Yuan, L.-S.; Huang, G.-P.; Wang, B. Quantitative investigation of multi-fracture morphology during TPDF through true tri-axial fracturing experiments and CT scanning. *Pet. Sci.* **2022**, *19*, 1700–1717. [CrossRef]
3. Peng, Y.; Zhao, J.; Sepehrnoori, K.; Li, Y.; Yu, W.; Zeng, J. Study of the Heat Transfer in the Wellbore During Acid/Hydraulic Fracturing Using a Semianalytical Transient Model. *SPE J.* **2019**, *24*, 877–890. [CrossRef]
4. Wang, J.; Zhou, F.; Bai, H.; Wei, D.; Ma, J.; Yang, P.; Zhang, F.; Yuan, L. A new approach to study the friction-reduction characteristics of viscous/conventional slickwater in simulated pipelines and fractures. *J. Nat. Gas Sci. Eng.* **2020**, *83*, 103620. [CrossRef]
5. Ahmadpour, V.; Mirzaei, I.; Rezazadeh, S.; Ahmadi, N. Investigation of solid/liquid interface evolution in the solidification process of liquid metal in an annulus crucible at the presence of static magnetic field: Numerical study. *J. Braz. Soc. Mech. Sci. Eng.* **2019**, *41*, 404. [CrossRef]
6. Liu, Z.; Reynolds, A.C. Gradient-Enhanced Support Vector Regression for Robust Life-Cycle Production Optimization with Nonlinear-State Constraints. *SPE J.* **2020**, *26*, 1590–1613. [CrossRef]
7. Li, M.; Lv, W.; Liu, J.; Sun, Z.; Zhou, F.; Wang, B. Effect of perforation friction on 3D In-stage multiple fracture propagation: A numerical study. *Eng. Fract. Mech.* **2022**, *267*, 108415. [CrossRef]
8. Peng, Y.; Zhao, J.; Sepehrnoori, K.; Li, Z.; Xu, F. Study of delayed creep fracture initiation and propagation based on semi-analytical fractional model. *Appl. Math. Model.* **2019**, *72*, 700–715. [CrossRef]
9. Du, J.; Guo, G.; Liu, P.; Xiong, G.; Chen, P.; Liu, J.; Chen, X. Experimental Study on the Autogenic Acid Fluid System of a High-Temperature Carbonate Reservoir by Acid Fracturing. *ACS Omega* **2022**, *7*, 12066–12075. [CrossRef]
10. Dong, R.; Wheeler, M.F.; Su, H.; Ma, K. Modeling Multistage Acid Fracturing Treatments in Carbonate Reservoirs. In Proceedings of the SPE Hydraulic Fracturing Technology Conference and Exhibition, Online, 4–6 May 2021. [CrossRef]
11. Zhang, K.; Chen, M.; Zhou, C.; Dai, Y.; Liu, F.; Li, J. Study of alternating acid fracturing treatment in carbonate formation based on true tri-axial experiment. *J. Pet. Sci. Eng.* **2020**, *192*, 107268. [CrossRef]
12. Li, M.; Zhou, F.; Sun, Z.; Dong, E.; Zhuang, X.; Yuan, L.; Wang, B. Experimental study on plugging performance and diverted fracture geometry during different temporary plugging and diverting fracturing in Jimusar shale. *J. Pet. Sci. Eng.* **2022**, *215*, 110580. [CrossRef]
13. Aljawad, M.S.; Aljulaih, H.; Mahmoud, M.; Desouky, M. Integration of field, laboratory, and modeling aspects of acid fracturing: A comprehensive review. *J. Pet. Sci. Eng.* **2019**, *181*, 106158. [CrossRef]
14. Gou, B.; Guan, C.; Li, X.; Ren, J.; Zeng, J.; Wu, L.; Guo, J. Acid-etching fracture morphology and conductivity for alternate stages of self-generating acid and gelled acid during acid-fracturing. *J. Pet. Sci. Eng.* **2021**, *200*, 108358. [CrossRef]
15. Nima, A.; Sajad, R.; Mirkazem, Y.; Iraj, M. Numerical investigation of species distribution and the effect of anode transfer coefficient on the proton exchange membrane fuel cell (PEMFC) performance. *Chem. Ind.* **2012**, *46*, 71. [CrossRef]
16. Zhang, R.; Hou, B.; Zhou, B.; Liu, Y.; Xiao, Y.; Zhang, K. Effect of acid fracturing on carbonate formation in southwest China based on experimental investigations. *J. Nat. Gas Sci. Eng.* **2019**, *73*, 103057. [CrossRef]
17. Lufeng, Z.; Fujian, Z.; Shicheng, Z.; Zhun, L.; Jin, W.; Yuechun, W. Evaluation of permeability damage caused by drilling and fracturing fluids in tight low permeability sandstone reservoirs. *J. Pet. Sci. Eng.* **2019**, *175*, 1122–1135. [CrossRef]
18. You, J.; Lee, K.J. Analyzing the Dynamics of Mineral Dissolution during Acid Fracturing by Pore-Scale Modeling of Acid-Rock Interaction. *SPE J.* **2021**, *26*, 639–652. [CrossRef]
19. Mehrjoo, H.; Norouzi-Apourvari, S.; Jalalifar, H.; Shajari, M. Experimental study and modeling of final fracture conductivity during acid fracturing. *J. Pet. Sci. Eng.* **2021**, *208*, 109192. [CrossRef]
20. Shah, M.; Agarwal, J.R.; Patel, D.; Chauhan, J.; Kaneria, D.; Shah, S.N. An assessment of chemical particulate technology as diverters for refracturing treatment. *J. Nat. Gas Sci. Eng.* **2020**, *84*, 103640. [CrossRef]
21. Gou, B.; Qin, N.; Wang, C.; Ren, J.; Guo, J.; Zeng, M.; Zhou, C.; Liu, F. Acidizing Model to Couple the Closure Stress and Acid-Rock Reactive Transport in Naturally Fractured Carbonate Reservoir. In Proceedings of the 55th U.S. Rock Mechanics/Geomechanics Symposium, Online, 18–25 June 2021. Available online: https://onepetro.org/ARMAUSRMS/proceedings/ARMA21/All-ARMA21/ARMA-2021-1221/467963 (accessed on 27 November 2021).
22. Liu, Z.; Reynolds, A. Robust Multiobjective Nonlinear Constrained Optimization with Ensemble Stochastic Gradient Sequential Quadratic Programming-Filter Algorithm. *SPE J.* **2021**, *26*, 1964–1979. [CrossRef]
23. Hosseinzadeh, B.; Bazargan, M.; Rostami, B.; Ayatollahi, S. Modeling of Wormhole Propagation in Carbonate Rocks by Use of In-Situ-Gelled Acids. *SPE J.* **2017**, *22*, 2032–2048. [CrossRef]
24. Zhang, L.; He, J.; Wang, H.; Li, Z.; Zhou, F.; Mou, J. Experimental investigation on wormhole propagation during foamed-VES acidizing. *J. Pet. Sci. Eng.* **2020**, *198*, 108139. [CrossRef]
25. Nasr-El-Din, H.A.; Al-Ghamdi, A.H.; Al-Qahtani, A.A.; Samuel, M.M. Impact of Acid Additives on the Rheological Properties of a Viscoelastic Surfactant and Their Influence on Field Application. *SPE J.* **2008**, *13*, 35–47. [CrossRef]
26. Rabie, A.I.; Gomaa, A.M.; Nasr-El-Din, H.A. Reaction of In-Situ-Gelled Acids With Calcite: Reaction-Rate Study. *SPE J.* **2011**, *16*, 981–992. [CrossRef]

27. Dong, R.; Wheeler, M.F.; Ma, K.; Su, H. A 3D Acid Transport Model for Acid Fracturing Treatments With Viscous Fingering. In Proceedings of the SPE Annual Technical Conference and Exhibition, Online, 26–29 October 2020. [CrossRef]
28. Wu, B.; Zhang, M.; Deng, W.; Que, J.; Liu, W.; Zhou, F.; Wang, Q.; Li, Y.; Liang, T. Study and Mechanism Analysis on Dynamic Shrinkage of Bottom Sediments in Salt Cavern Gas Storage. *Processes* **2022**, *10*, 1511. [CrossRef]
29. Li, Y.; Zhou, F.; Wang, J.; Li, B.; Xu, H.; Yao, E.; Zhao, L. Influence of Nanoemulsion Droplet Size of Removing Water Blocking Damage in Tight Gas Reservoir. *Energies* **2022**, *15*, 5283. [CrossRef]
30. Li, Y.; Zhou, F.; Li, B.; Cheng, T.; Zhang, M.; Wang, Q.; Yao, E.; Liang, T. Optimization of Fracturing Fluid and Retarded Acid for Stimulating Tight Naturally Fractured Bedrock Reservoirs. *ACS Omega* **2022**, *7*, 25122–25131. [CrossRef]